Article

Shape-Persistant Macrocycles with Terpyridine Units: Synthesis, Characterization, and Structure in the Crystal

Christian Grave, Dieter Lentz, Andreas Schfer, Paolo Samor, Jrgen P. Rabe, Peter Franke, and A. Dieter Schlter

J. Am. Chem. Soc., **2003**, 125 (23), 6907-6918• DOI: 10.1021/ja034029p • Publication Date (Web): 17 May 2003

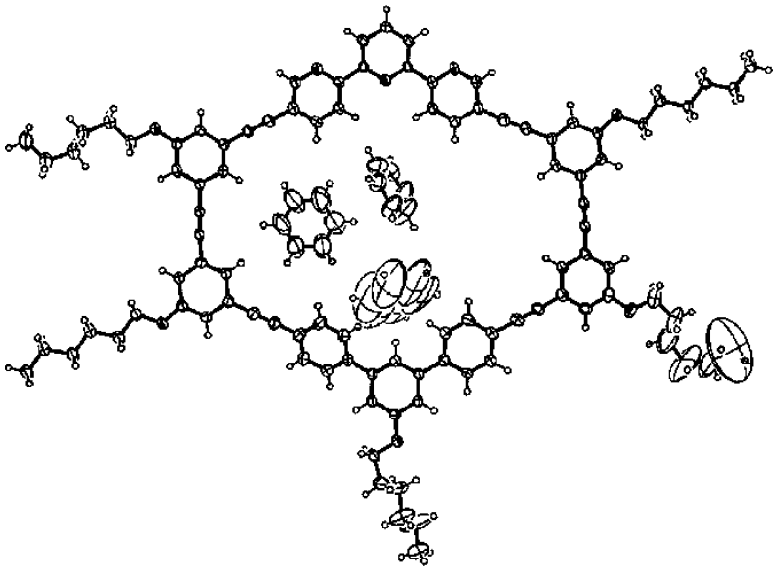

J|A|C|S
ARTICLES
Published on Web 05/17/2003

Shape-Persistant Macrocycles with Terpyridine Units: Synthesis, Characterization, and Structure in the Crystal

Christian Grave,[†] Dieter Lentz,*[,†] Andreas Schäfer,[†] Paolo Samorì,[‡,§] Jürgen P. Rabe,[‡] Peter Franke,[†] and A. Dieter Schlüter*[,†]

Institut für Chemie, Freie Universität Berlin, Takustrasse 3, D-14195 Berlin, Germany, and Institut für Physik, Humboldt Universität zu Berlin, Newtonstrasse 15 D-12489 Berlin, Germany

Received January 3, 2003; E-mail: adschlue@chemie.fu-berlin.de

Abstract: The synthesis of a variety of shape-persistent macrocycles with either one (**1a**−**d**, **2**) or two (opposing) terpyridine units (**3**, **4**, **5a**−**c**) and inner diameters of up to 2 nm is described. The sequences are mainly based on transition metal cross-coupling reactions and, whenever appropriate, compared with one another regarding their respective efficiency. Typical overall yields and amounts prepared range from 8% (**4**) to 27% (**3**) and 25 mg (**1a**) to 290 mg (**1b**), respectively. For solubility and processing of the targeted cycles, all precursors have already been decorated with flexible side chains (hexyloxy or hexyloxymethyl). The cycles' characterization is based on MALDI-TOF mass spectrometry, 2D NMR spectroscopy, and/or low-temperature single-crystal X-ray diffraction. Their packing in the crystal is discussed in terms of both number and length of side chains. Cycle **1d** was physisorbed into an ordered structure at the solution−HOPG interface and investigated by scanning tunneling microscopy (STM).

Introduction

In the last decade there was a great deal of research on shape-persistent macrocycles on the nanometer scale.[1,2] In contrast to flexible macrocycles such as cycloalkanes[3] their cyclic backbones' conformational rigidity creates a defined interior that is well separated from an exterior. This rigidity together with a noncollapsable and, thus, usable interior are the main factors that render these macrocycles interesting candidates for various supramolecular aspects/applications including lyotropic and thermotropic behavior,[4] organization into and transport through porous molecular crystals,[1a−c,5] and pattern formation at interfaces.[1d,6] Besides representatives such as cyclodextrins,[1e,7] cyclopeptides,[1f,8] metalacycles,[1g−i,9] etc.,[2a,b] macrocycles, especially with backbones consisting of only sp- or sp^2-hybridized atoms, have attracted considerable interest.[1a,c,d,j−w,2c,10] Moore's trailblazing phenylene acetylene macrocycles,[11] as well as

[†] Freie Universität Berlin.

[‡] Humboldt Universität zu Berlin.

[§] New address: Istituto per la Sintesi Organica e la Fotoreattività, CNR Bologna, Via Gobetti 101, 40129 Bologna, Italy.

(1) For a selection of the most recent examples, see: (a) Henze, O.; Lentz, D.; Schäfer, A.; Franke, P.; Schlüter, A. D. *Chem. Eur. J.* **2002**, 357−365. (b) Werz, T. B.; Staeb, T. H.; Benisch, C.; Rausch, B. J.; Rominger, F.; Gleiter, R. *Org. Lett.* **2002**, *4*, 339−342. (c) Campbell, K.; Kuehl, C. J.; Ferguson, M. J.; Stang, P. J.; Tykwinski, R. R. *J. Am. Chem. Soc.* **2002**, *124*, 7266−7267. (d) Bäuerle, P.; Mena-Osteritz, E.; Fuhrmann, G.; Kaiser, A.; Ammann, M. *Polym. Mater. Sci. Eng.* **2002**, *86*, 34. (e) Wakao, M.; Fukase, K.; Kusumoto, S. *J. Org. Chem.* **2002**, *67*, 8182−8190. (f) Sanderson, J. M.; Yazdani, S. *Chem. Commun.* **2002**, 1154−1155. (g) Newkome, G. R.; Cho, T. J.; Moorefield, C. N.; Cush, R.; Russo, P. S.; Godinez, L. A.; Saunders: M. J.; Mohapatra, P. *Chem. Eur. J.* **2002**, *8*, 2946−2954. (h) Schweiger, M.; Seidel, S. R.; Arif, A. M.; Stang, P. J. *Inorg. Chem.* **2002**, *41*, 2556−2559. (i) Takahashi, R.; Kobuke, Y. *J. Am. Chem. Soc.* **2003**, *125*, 2372−2373. (j) Iyoda, M.; Nakao, K.; Kondo, T.; Kuwatani, Y.; Yoshida, M.; Matsuyama, H.; Fukami, K.; Nagase, S. *Tetrahedron Lett.* **2001**, *42*, 6869−6872. (k) Campbell, K.; McDonald, R.; Ferguson, M. J.; Tykwinski, R. R. *Organometallics* **2003**, *22*, 1353−1355. (l) Schmittel, M.; Ganz, A.; Fenske, D. *Org. Lett.* **2002**, *4*, 2289−2292. (m) Baxter, P. N. W., *Chem. Eur. J.* **2002**, *8*, 5250−5264. (n) Yu, L.; Lindsey, J. S. *J. Org. Chem.* **2001**, *66*, 7402−7419. (o) Rucareanu, S.; Mongin, O.; Schuwey, A.; Hoyler, N.; Gossauer, A.; Amrein, W.; Hediger, H.-U. *J. Org. Chem.* **2001**, *66*, 4973−4988. (p) Schafer, L. L.; Nitschke, J. R.; Mao, S. S. H.; Liu, F.-Q.; Harder, G.; Haufe, M.; Tilley, T. D. *Chem. Eur. J.* **2002**, *8*, 74−83. (q) Tobe, Y.; Utsumi, N.; Kawabata, K.; Nagano, A.; Adachi, K.; Araki, S.; Sonoda, M.; Hirose, K.; Naemura, K. *J. Am. Chem. Soc.* **2002**, *124*, 5350−5364. (r) Nielsen, M. B.; Diederich, F. *Chem. Rec.* **2002**, *2*, 189−198. (s) Fischer, M.; Höger, S. *Eur. J. Org. Chem.* **2003**, 441−446. (t) Liu, C.-H.; Tour, J. *J. Org. Chem.* **2002**, *67*, 7761−7768. (u) An, D. L.; Nakano, T.; Orita, A.; Otera, J. *Angew. Chem., Int. Ed.* **2002**, *41*, 171−173. (v) Srinivasan, M.; Sankararaman, S.; Hopf, H.; Varghese, B. *Eur. J. Org. Chem.* **2003**, 660−665. (w) Shen, X.; Ho, D. M.; Pascal, R. A., Jr. *Org. Lett.* **2003**, *5*, 369−371. (x) Chiu, S.-H.; Pease, A. R.; Stoddart, J. F.; White, A. J. P.; Williams, D. J. *Angew. Chem., Int. Ed.* **2002**, *41*, 270−274. (y) de Meijere, A.; Kozhushkov, S. I. *Chem. Eur. J.* **2002**, *8*, 3195−3202. (z) Higuchi, M.; Kanazawa, H.; Yamamoto, K. *Org. Lett.* **2003**, *5*, 345−347.

(2) For recent reviews, see: (a) de Meijere, A.; Kozhushkov, S. I. *Top. Curr. Chem.* **1999**, *201*, 1−42. (b) Höger, S. *J. Polym. Sci., Part A: Polym. Chem.* **1999**, *37*, 2685−2698. (c) Grave, C.; Schlüter, A. D. *Eur. J. Org. Chem.* **2002**, 3075−3098.

(3) See, for example: Keul, H.; Höcker, H. Cycloalkanes and Related Oligomers and Polymers. In *Large Ring Molecules*; Semlyen, J. A., Ed.; J. Wiley & Sons: Chichester, 1996; Chapter 10, pp 375−406.

(4) See, for example: (a) Kimura, M.; Wada, K.; Ohta, K.; Hanabusa, K.; Shirai, H.; Kobayashi, N. *J. Am. Chem. Soc.* **2001**, *123*, 2438−2439. (b) Höger, S.; Enkelmann, V.; Bonrad, K.; Tschierske, C. *Angew. Chem., Int. Ed.* **2000**, *39*, 2268−2270. (c) Mindyuk, O. Y.; Stetzer, M. R.; Heiney, P. A.; Nelson, J. C.; Moore, J. S. *Adv. Mater.* **1998**, *10*, 1363−1366.

(5) See, for example: (a) Müller, P.; Usón, I.; Hensel, V.; Schlüter, A. D.; Sheldrick, G. M. *Helv. Chim. Acta* **2001**, *84*, 778−785. (b) Venkataraman, D.; Lee, S.; Zhang, J.; Moore, J. S. *Nature* **1994**, *371*, 591−593.

(6) See, for example: (a) Höger, S.; Bonrad, K.; Mourran, A.; Beginn, U.; Möller, M. *J. Am. Chem. Soc.* **2001**, *123*, 5651−5659. (b) Krömer, J.; Rios-Carreras, I.; Fuhrmann, G.; Musch, C.; Wunderlin, M.; Debaerdemaeker, T.; Mena-Osteritz, E.; Bäuerle, P. *Angew. Chem., Int. Ed.* **2000**, *112*, 3623−3628. (c) Mindyuk, O. Y.; Stetzer, M. R.; Gidalevitz, D.; Heiney, P. A.; Nelson, J. C.; Moore, J. S. *Langmuir* **1999**, *15*, 6897−6900.

(7) Harada, A. Cyclodextrins. In *Large Ring Molecules*; Semlyen, J. A., Ed.; J. Wiley & Sons: Chichester, 1996; Chapter 11, pp 407−432.

(8) Scheraga, H. A. Cyclic Peptides and Loops in Proteins. In *Large Ring Molecules*; Semlyen, J. A., Ed.; J. Wiley & Sons: Chichester, 1996; Chapter 3, pp 99−112.

(9) Leininger, S.; Olenyuk, B.; Stang, P. J. *Chem. Rev.* **2000**, *100*, 853−908.

phenylene[12] and phenylene butadiynylene ones,[13] are the basic structural types here. They have been described in sizes of up to approximately 3 nm (diameter) and with different side-chain patterns.[2]

There has recently been a tendency to extend the field of shape-persistent and nanosized macrocycles to those with exo- or endocyclically oriented heteroatoms as anchor groups.[1a,c,d,j−p,2c] The incorporation of anchor groups such as sulfur in thiophene[1d,j,6b] or the nitrogens in pyridine,[14] bipyridines,[1a,15] and terpyridines[16] widens the cycles' applicability considerably. Macrocycles with exocyclically oriented anchor sites may be used, for example, as rigid scaffolds to hold metals at a defined distance[1c,17] or for metal-mediated linear (1D), areal (2D), or even spatial (3D) constructs in which the cycles serve as Tinkertoy building blocks and the metals as connectors.[1c,l] Endocyclic anchor groups, in turn, should allow one to either specifically bind guests inside a cycle's cavity[1m−o,s,18] or induce incorporation of, for example, metal clusters. In combination with the cycles' presumed inherent ability to form superstructures with channels by aggregation, these thoughts could lead to a new approach to atomically thin metal wires.[19]

2,2′-Bipyridine and 2,2′:6′,2″-terpyridine are widely used as ligands for metal complexation;[20] these complexes show interesting photophysical and electrochemical properties.[21] Their incorporation into macrocyclic backbones may suit especially well the purposes described above. We have synthesized, therefore, a number of 5,5′-substituted bi- and 5,5″-substituted terpyridine building blocks[22] for the construction of shape-persistent macrocycles, a few of which have already been obtained.[1a,15,16] The present contribution describes the synthesis of a whole set of phenylacetylene macrocycles with either one or two terpyridine units. They differ in size and side-chain pattern. To provide a solid basis for a systematic exploration of their supramolecular and materials chemistry related properties, the optimum synthesis strategy and the availability are discussed in some detail. Solubility is an essential feature for characterization and processing of conformationally rigid compounds. For some of these cycles, the solubilities in chloroform were quantified, therefore, and qualitatively correlated with structural factors such as side-chain pattern and number of terpyridine units per cycle. Furthermore, first insights into these cycles' packing behavior both in the 3D of a single crystal and in the 2D of self-assembled monolayers adsorbed on highly oriented pyrrolytic graphite (HOPG) are provided by X-ray diffraction and scanning tunneling microscopy investigations, respectively.

Results and Discussion

Synthesis. The target structures reported here are hexagonal and carry either 46 (**1a**−**d**, **3**), 50 (**4**), or 58 (**2**, **5a**−**c**) atoms in the core, thus being the largest shape-persistent pyridine-containing macrocycles described so far (Figure 1).[14,16] To allow a stepwise approach to metal complexes, cycles with either one or two terpyridine units were prepared. In the former case the terphenyl unit serves as a geometrically similar placeholder for terpyridyl. The different side-chain patterns ought to mediate solubility and influence aggregation behavior. The tetrahydropyranyl (THP) groups in **1c** and **5b** serve as protecting groups for OH to allow easy modifications on an already existing macrocycle without having to carry the modification through parts of the sequence. Except **4**, which was cyclized via oxidative alkynyl−alkynyl homocoupling,[23] all other structures were cyclized via Sonogashira (alkynyl−aryl) cross-coupling.[24]

An aspect to be considered in macrocyclic chemistry is the number of precursor compounds that are used in the final cyclization step. The more of them employed, the lower the cyclization yield will normally be, but their syntheses' effort will also decrease. In contrast, the fewer precursors used, the higher their syntheses' effort will be and cyclization efficiency will normally increase. For each individual cycle the efficiency maximum of these two opposing effects has to be individually assessed. From a comprehensive evaluation of the literature, by and large, one can conclude that regarding cycles containing heteroaromatic units (like terpyridenes) a cyclization strategy involving two cyclization precursors seems to be the optimum.[2c] Equipped with AA and BB functionalities, respectively, they lead to cycles in yields of 20−25% irrespective of whether the two "halves" have similar sizes or not. Considerations to generate heteroaromatic cycles from just one precursor compound (which obviously must be of the AB-type) are synthetically unattractive, because, for the cases considered here, this would require appropriately unsymmetrically functionalized terpyridines. They, however, do not exist yet.[25,26] The target

(10) For a highlight on "polyunsaturated cyclophanes", see: Bodwell, G. J.; Satou, T. *Angew. Chem., Int. Ed.* **2002**, *41*, 4003−4007.
(11) Zhang, J.; Pesak, D. J.; Ludwick, J. L.; Moore, J. S. *J. Am. Chem. Soc.* **1994**, *116*, 4227−4239.
(12) (a) Hensel, V.; Schlüter, A. D. *Chem. Eur. J.* **1999**, *5*, 421−429. (b) Schlüter, A. D.; Hensel, V.; Liess, P.; Lützow, K. *NATO ASI Series, Series C: Mathematical and Physical Sciences* (**1999**), *499* (Modular Chemistry), 241−250. (c) Hensel, V.; Lützow, K.; Jacob, J.; Gessler, K.; Saenger, W.; Schlüter, A. D. *Angew. Chem., Int. Ed. Engl.* **1997**, *36*, 2654−2656.
(13) (a) Tobe, Y.; Utsumi, N.; Nagano, A.; Naemura, K. *Angew. Chem., Int. Ed.* **1998**, *37*, 1285−1287. (b) Höger, S.; Meckenstock, A.-D.; Pellen, H. *J. Org. Chem.* **1997**, *62*, 4556−4557. (c) de Meijere, A.; Kozhushkov, S.; Haumann, T., Boese, R.; Puls, C.; Cooney, M. J.; Scott, L. T. *Chem. Eur. J.* **1995**, *1*, 124. (d) Boldi, A. M.; Diederich, F. *Angew. Chem., Int. Ed. Engl.* **1994**, *33*, 486. (e) Anderson, H. L.; Sanders, J. K. M. *Angew. Chem., Int. Ed. Engl.* **1990**, *29*, 1400−1403.
(14) Tobe, Y.; Nagano, A.; Kawabata, K.; Sonoda, M.; Naemura, K. *Org. Lett.* **2000**, *2*, 3265−3268.
(15) Henze, O.; Lentz, D.; Schlüter, A. D. *Chem. Eur. J.* **2000**, 2362−2367.
(16) Lehmann, U.; Schlüter, A. D. *Eur. J. Org. Chem.* **2000**, 3483−3487.
(17) Campbell, K.; McDonald, R.; Tykwinski, R. R. *J. Org. Chem.* **2002**, *67*, 1133−1140.
(18) Nakash, M.; Sanders, J. K. M. *J. Chem. Soc., Perkin Trans. 2* **2001**, 2189−2194.
(19) See, for example: (a) Hong, B. H.; Bae, S. C.; Lee, C.-W.; Jeong, S.; Kim, K. S. *Science* **2001**, *294*, 348−351. (b) Gudiksen, M. S.; Lauhorn, L. J.; Wang, J.; Smith, D. C.; Lieber, C. M. *Nature* **2002**, *415*, 617−620.
(20) For related reviews see: (a) Schubert, U. S.; Eschbaumer, C. *Angew. Chem., Int. Ed.* **2002**, *41*, 2892−2926. (b) Kaes, C.; Katz, A.; Hosseini, M. W. *Chem. Rev.* **2000**, *100*, 3553−3590. (c) Cargill Thompson, A. M. W. *Coord. Chem. Rev.* **1997**, *160*, 1−52. (d) Constable, E. C. *Adv. Inorg. Chem. Radiochem.* **1986**, *30*, 69−121.
(21) Sauvage, J.-P.; Collin, J.-P.; Chambron, J.-C.; Guillerez, S.; Coudret, C.; Balzani, V.; Barigelletti, F.; DeCola, L.; Flamigni, L. *Chem. Rev.* **1994**, *94*, 993−1019.
(22) (a) Manickam, G.; Schlüter, A. D. *Synthesis* **2000**, *3*, 442−446. (b) Manickam, G.; Schlüter, A. D. *Eur. J. Org. Chem.* **2000**, 3475−3481. (c) Henze, O.; Lehmann, U.; Schlüter, A. D. *Synthesis* **1999**, *4*, 683−687. (d) Lehmann, U.; Henze, O.; Schlüter, A. D. *Chem. Eur. J.* **1999**, *5*, 854−859.
(23) For oxidative alkynyl−alkynyl homocoupling reactions catalyzed by Pd^{2+}, see, for example: (a) Liu, Q.; Burton, D. J. *Tetrahedron Lett.* **1997**, *38*, 4371−4374. (b) Takano, S.; Sugihara, T.; Ogasawara, K. *Synlett* **1990**, 453−454. (c) Rossi, R.; Carpita, A.; Bigelli, C. *Tetrahedron Lett.* **1985**, *26*, 523−526.
(24) (a) Sonogashira, K. *Coupling Reactions Between sp^2 and sp Carbon Centers* in *Comprehensive Organic Synthesis*; Trost, B. M., Ed.; Pergamon: New York, 1991; Vol 3, Chapter 2.4. (b) Sonogashira, K.; Thoda, Y.; Hagihara, N. *Tetrahedron Lett.* **1975**, *16*, 4467−4470.
(25) For a recent review about unsymmetrical bi- and terpyridines, see: Chelucci, G.; Thummel, R. P. *Chem. Rev.* **2002**, *102*, 3129−3170.
(26) For a procedure to generate an unsymmetrically functionalized phenanthroline building block for a similar purpose, see: Liu, S.-X.; Michel, C.; Schmittel, M. *Org. Lett.* **2000**, *2*, 3959−3962.

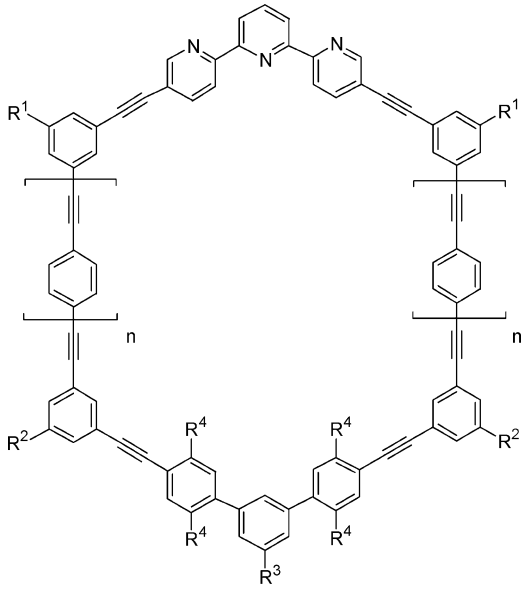

	n	R^1	R^2	R^3	R^4
1a	0	OC_6H_{13}	OC_6H_{13}	OC_6H_{13}	H
1b	0	$CH_2OC_6H_{13}$	$CH_2OC_6H_{13}$	OC_6H_{13}	H
1c	0	$CH_2OC_6H_{13}$	CH_2OTHP	OC_6H_{13}	H
1d	0	OC_6H_{13}	OC_6H_{13}	H	C_6H_{13}
2	1	$CH_2OC_6H_{13}$	$CH_2OC_6H_{13}$	OC_6H_{13}	H

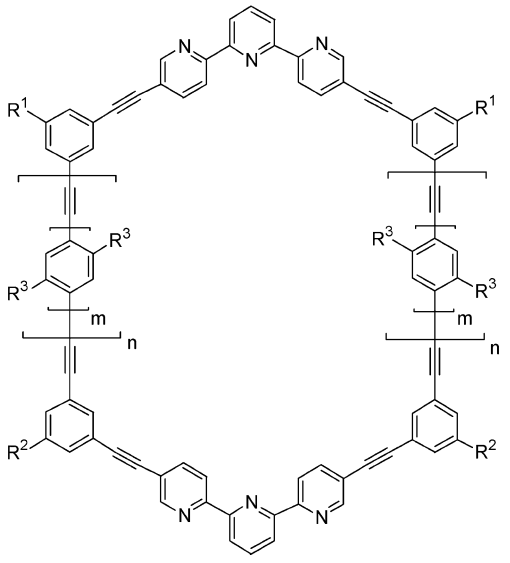

	n	m	R^1	R^2	R^3
3	0	0	$CH_2OC_6H_{13}$	$CH_2OC_6H_{13}$	-
4	1	0	$CH_2OC_6H_{13}$	$CH_2OC_6H_{13}$	-
5a	1	1	$CH_2OC_6H_{13}$	$CH_2OC_6H_{13}$	H
5b	1	1	$CH_2OC_6H_{13}$	CH_2OTHP	H
5c	1	1	$CH_2OC_6H_{13}$	$CH_2OC_6H_{13}$	C_6H_{13}

Figure 1. Synthesized macrocycles with one (**1**, **2**) or two terpyridine units (**3**−**5**).

structures presented in Figure 1 were, therefore, accessed by cyclization of AA- and BB-type "half-ring" precursors with either a terphenyl or terpyridine unit.

Scheme 1. Stepwise Synthesis of Terpyridine Unit **14a**[a]

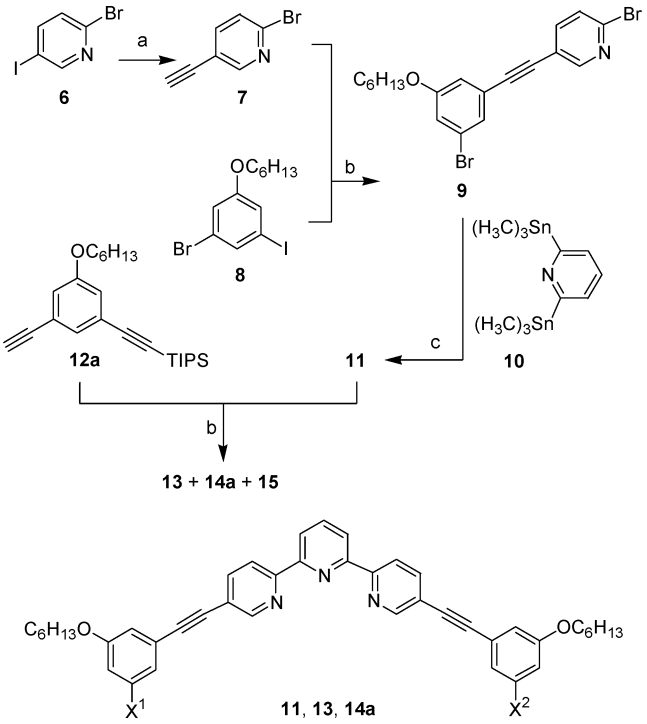

	X^1	X^2	Yield
7	-	-	81 %
9	-	-	82 %
11	Br	Br	58 %
13	Br	R	42-46 % (GPC)
14a	R	R	49-55 % (GPC)

15: R-R

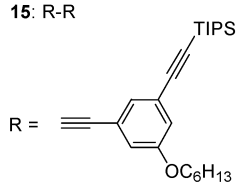

[a] Reagents and conditions: (a) 1. TMS-acetylene, $Pd(PPh_3)_4$/CuI, TEA/toluene; 2. MeOH, (b) $Pd(PPh_3)_4$/CuI, TEA/toluene, and (c) $Pd(PPh_3)_4$, toluene.

Due to the lower symmetry of macrocycles with heteroaromatic units, repetitive strategies toward the precursor molecules that otherwise proved to be very useful in macrocycle synthesis[11,12] are not feasible here. The cycles' smallest repeat unit (if there are any) has already the size of a cyclization precursor. The alternative building block strategy for a modular approach to two half-ring precursors has been successfully employed.[1a,15,16]

The synthetic sequences to the cycles **1**−**5** are divided into Schemes 1−7. Scheme 1 describes a stepwise construction of the symmetrical cycle precursor **14a** with an early generation of the terpyridine unit (in **11**), Scheme 2 a more favorable synthesis of **14** and some derivatives with a late generation of the terpyridine unit (in **14**), Scheme 3 the assembly of cycles **1a**−**d** from the differently sized "half-rings" **20a**−**c** as AA-type and **21a**,**b** as BB-type components, respectively, Scheme 4 the assembly of the large precursor **26b**, again with a late generation of the terpyridine unit (in **26a**), and its cyclization with the BB-type component **21a** to the cycle **2**, Scheme 5 the assembly of cycle **3** from the two similarly sized half-rings **30** as AA-type and **33b** as BB-type component with an early generation of the terpyridine, Scheme 6 the analogous assembly of the larger cycles **5a**−**c** from precursors **33b**,**c** and **35a**,**b**, and, finally, Scheme 7 the oxidative cyclization of the half-ring precursor **33b** to cycle **4**. In the following the different synthesis parts will be briefly commented on.

Scheme 2. Synthesis of Half-Rings **20a**−**c** with the Terpyridine Assembly in the Last Step[a]

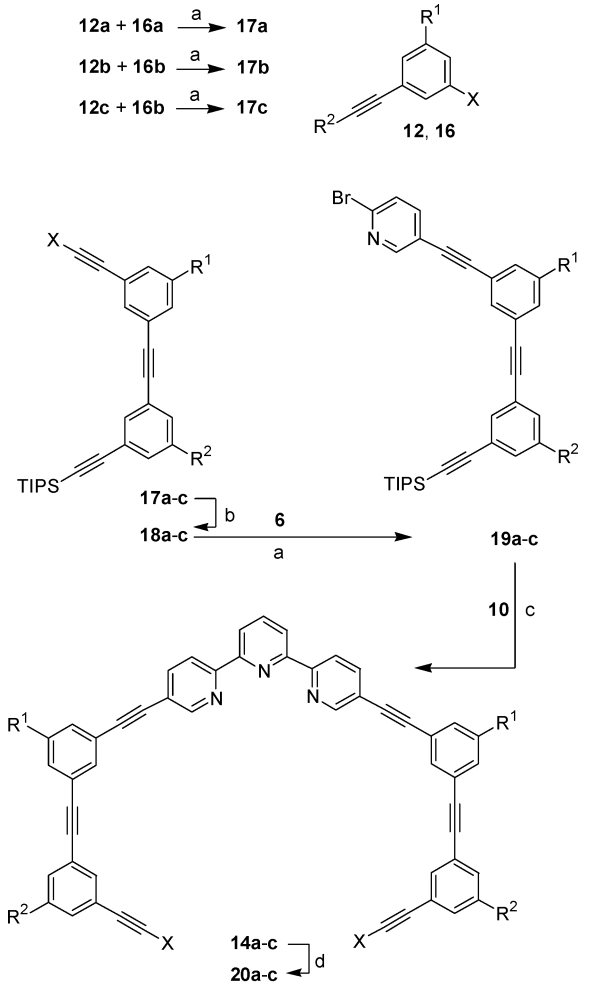

	R^1	R^2	X	Yield
12a	OC_6H_{13}	TIPS	CCH	-
12b	$CH_2OC_6H_{13}$	TIPS	CCH	-
12c	CH_2OTHP	TIPS	CCH	-
16a	OC_6H_{13}	TMS	Br	-
16b	$CH_2OC_6H_{13}$	TMS	Br	-
14a	OC_6H_{13}	OC_6H_{13}	TIPS	43 %
14b	$CH_2OC_6H_{13}$	$CH_2OC_6H_{13}$	TIPS	55 %
14c	$CH_2OC_6H_{13}$	CH_2OTHP	TIPS	31 %
17a	OC_6H_{13}	OC_6H_{13}	TMS	75 %
17b	$CH_2OC_6H_{13}$	$CH_2OC_6H_{13}$	TMS	76 %
17c	$CH_2OC_6H_{13}$	CH_2OTHP	TMS	61 %
18a	OC_6H_{13}	OC_6H_{13}	H	98 %
18b	$CH_2OC_6H_{13}$	$CH_2OC_6H_{13}$	H	97 %
18c	$CH_2OC_6H_{13}$	CH_2OTHP	H	86 %
19a	OC_6H_{13}	OC_6H_{13}	-	88 %
19b	$CH_2OC_6H_{13}$	$CH_2OC_6H_{13}$	-	73 %
19c	$CH_2OC_6H_{13}$	CH_2OTHP	-	93 %
20a	OC_6H_{13}	OC_6H_{13}	H	82 %
20b	$CH_2OC_6H_{13}$	$CH_2OC_6H_{13}$	H	84 %
20c	$CH_2OC_6H_{13}$	CH_2OTHP	H	93 %

[a] Reagents and conditions: (a) $Pd(PPh_3)_4$/CuI, TEA; (b) NaOH, methanol/CH_2Cl_2; (c) $Pd(PPh_3)_4$, toluene; and (d) Bu_4NF, THF.

Scheme 3. Ring-Closure of 46-Membered Cycles **1a**−**d** with One Terpyridine Unit[a]

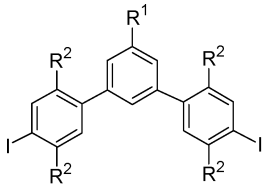

	R^1	R^2
21a	OC_6H_{13}	H
21b	H	C_6H_{13}

20a + **21a** → **1a**, 21 % + $[\mathbf{1a}]_2$, 12 %
20b + **21a** → **1b**, 21 % + $[\mathbf{1b}]_2$, 9 %
20c + **21a** → **1c**, 18 % + $[\mathbf{1c}]_2$, 5 %
20a + **21b** → **1d**, 17 %

[a] Reagents and conditions: $Pd(PPh_3)_4$/CuI, TEA/toluene, high dilution.

Scheme 1. The iodobromopyridine **6** was coupled with TMS−acetylene under Sonogashira conditions. One-pot deprotection and recrystallization yielded the bromo,ethynyl-functionalized pyridine **7**. Its reaction with the bromoiodobenzene **8** under Sonogashira conditions gave product **9** by selective coupling at the iodo site of **8**, thus leaving the two bromo functions of both coupling partners unaffected. In analogy to a known terpyridine synthesis[22d] the pyridyl bromo function of **9** was then reacted under Stille cross-coupling conditions with bis-stannylated pyridine **10** to selectively give terpyridine **11**. Some bipyridine homocoupling product was removed during isolation. The bis-stannylated pyridine **10** is a key compound in the present work.[27] All terpyridines reported here were synthesized by coupling it with an ethynyl-substituted bromofunctionalized pyridine (**9**, **19a**−**c**, **25**, **27**, **31a**−**c**). The yields of the respective products (**11**, **14a**−**c**, **26a**, **28a**, **32a**−**c**) vary between 31 and 70%, with a tendency to decreasing values for increasing substituent's size of the bromo pyridine. The reported yields of terpyridines prepared by the same strategy depend on the substitution of the pyridines used and at 14−55% are somewhat lower.[16,22d,28] Sonogashira cross-coupling of **11** with ethynyl compound **12a** gave a mixture of the desired product **14a**, starting material **11**, monocoupled **13**, and the homocoupled **15**, with the separation of the former three being extremely tedious and associated with an enormous loss of material, although after several columns pure **14a** could finally be obtained. Different conditions (DIPEA/toluene or propylamine) did not improve the results. Thus, the relatively early generation of the terpyridine unit in the sequence was considered disadvantageous as long as the separation problem could not be solved. Possible ways to solve the problem would be either the application of a larger excess of **12a** or the transformation of bromo into the much more reactive iodo functionality. The former was unattractive because **12**'s synthesis involves six steps and its recovery was expected to be too complicated due to homocoupling side reactions. The latter option was also not seriously considered because of the known incompatibility of the terpyridine unit with many iodination reagents.[29] We, therefore, decided to move the generation of the terpyridine unit

(27) Yamamoto, Y.; Yanagi, A. *Chem. Pharm. Bull.* **1982**, *30*, 1731−1737.
(28) For a recent, improved synthetic method via a central 2,6-diiodopyridine building block, see: Colasson, B. X.; Dietrich-Buchecker, C.; Sauvage, J.-P. *Synlett* **2002**, 271−272.
(29) See, for example: (a) Henze, O. Ph.D. Thesis, FU Berlin, Germany, 2000, http://www.diss.fu-berlin.de/2000/47/. (b) Lehmann, U. Ph.D. Thesis, FU Berlin, Germany, 1999.

Scheme 4. Synthesis of 58-Membered Cycle **2** with One Terpyridine Unit[a]

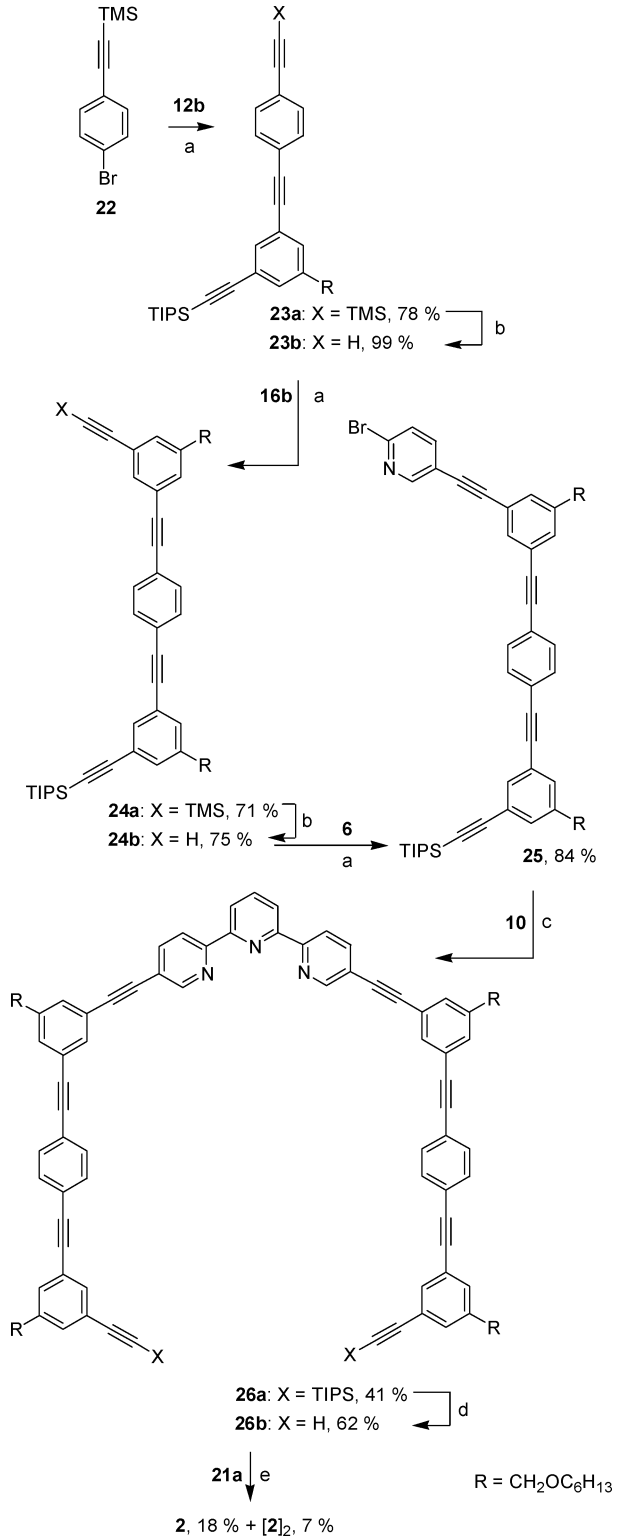

[a] Reagents and conditions: (a) $Pd(PPh_3)_4$/CuI, TEA; (b) NaOH, methanol/CH_2Cl_2; (c) $Pd(PPh_3)_4$, toluene; (d) Bu_4NF, THF; and (e) $Pd(PPh_3)_4$/CuI, TEA, high dilution.

to the latest possible step and, in the case of incomplete terpyridine formation, exploit the polarity differences of main and side products for an easy separation. Another strategy that avoids different side products with terpyridine units is available[30] but was not applied in the context of the present work.

Scheme 5. Synthesis of 46-Membered Cycle **3** with Two Terpyridine Units[a]

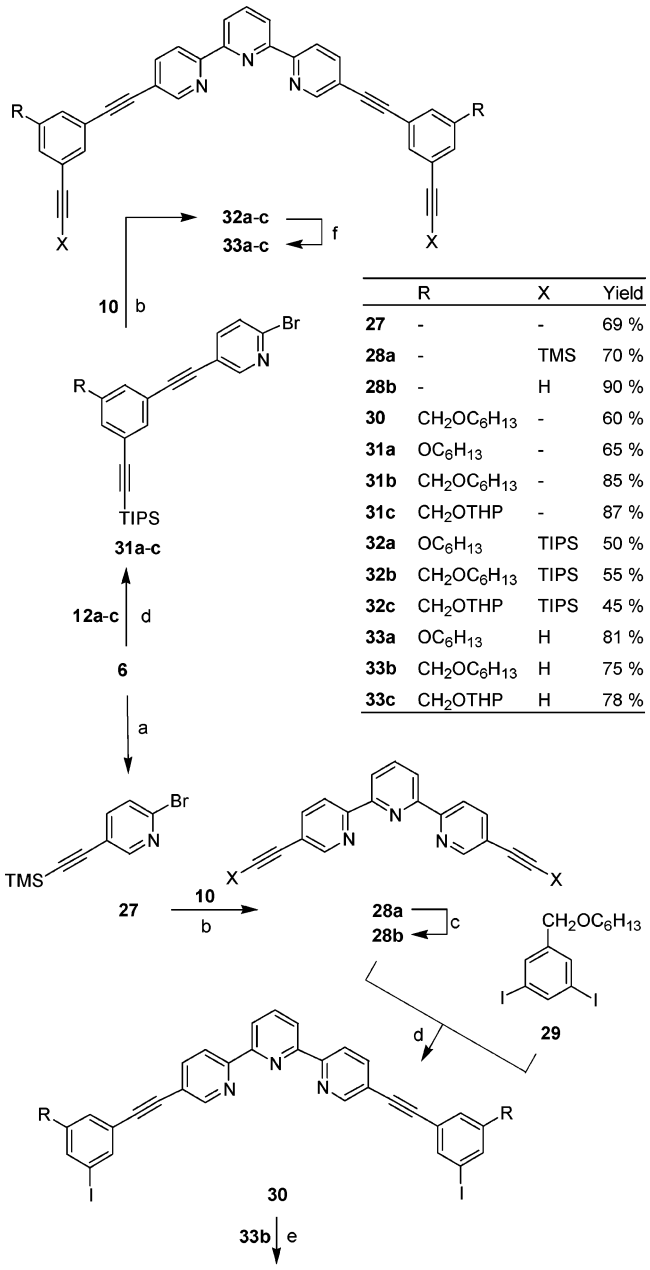

	R	X	Yield
27	-	-	69 %
28a	-	TMS	70 %
28b	-	H	90 %
30	$CH_2OC_6H_{13}$	-	60 %
31a	OC_6H_{13}	-	65 %
31b	$CH_2OC_6H_{13}$	-	85 %
31c	CH_2OTHP	-	87 %
32a	OC_6H_{13}	TIPS	50 %
32b	$CH_2OC_6H_{13}$	TIPS	55 %
32c	CH_2OTHP	TIPS	45 %
33a	OC_6H_{13}	H	81 %
33b	$CH_2OC_6H_{13}$	H	75 %
33c	CH_2OTHP	H	78 %

[a] Reagents and conditions: (a) $Pd(PPh_3)_4$/CuI, TMS-acetylene, TEA/toluene; (b) $Pd(PPh_3)_4$, toluene; (c) NaOH, methanol/CH_2Cl_2; (d) $Pd(PPh_3)_4$/CuI, TEA, or TEA/toluene; (e) $Pd(PPh_3)_4$/CuI, TEA/toluene, high dilution; and (f) Bu_4NF, THF.

Scheme 2. The alternative sequence has the same number of reaction steps. Here first the pyridines **19a**−**c**, which already contain one complete side and two corners, were generated via a series of coupling/deprotection steps. Then the terpyridine unit was assembled by reacting these pyridines with the bisstannyl **10** to give **14a**−**c**, respectively, in yields from 31 to 55%. Their purification from monocoupled side product and homocoupled bipyridine was easily possible due to the large enough difference in polarity between these compounds with different numbers of pyridyl substituents.

(30) Grave, C. Ph.D. Thesis, FU Berlin, Germany, 2002, http://www.diss.fu-berlin.de/2002/156/.

Scheme 6. Synthesis of 58-Membered Cycles **5a**−**c** with Two Terpyridine Units[a]

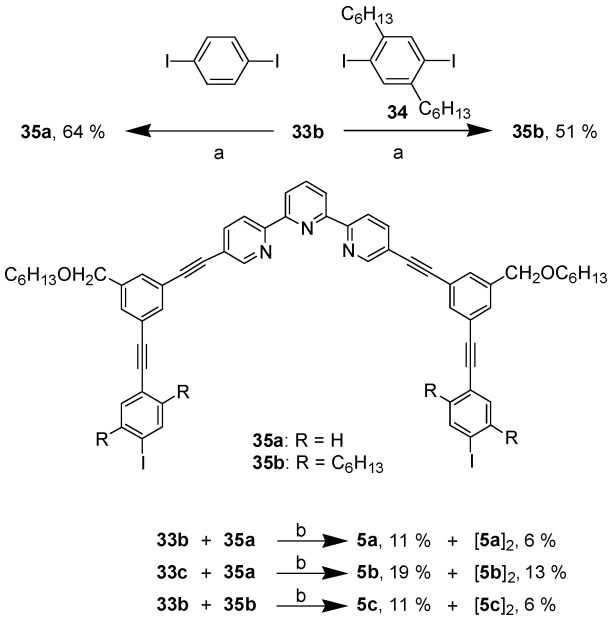

33b + **35a** → (b) **5a**, 11 % + [**5a**]$_2$, 6 %
33c + **35a** → (b) **5b**, 19 % + [**5b**]$_2$, 13 %
33b + **35b** → (b) **5c**, 11 % + [**5c**]$_2$, 6 %

[a] Reagents and conditions: (a) Pd(PPh$_3$)$_4$/CuI, TEA/toluene and (b) Pd(PPh$_3$)$_4$/CuI, TEA/toluene, high dilution.

Scheme 7. Synthesis of 40-Membered Cycle **4** by Oxidative Alkynyl−Alkynyl Coupling[a]

33b → **4**, 8 % + [**4**]$_2$, 3 %

[a] Conditions: Pd(PPh$_3$)$_2$Cl$_2$/CuI, O$_2$, THF/piperidine, pseudo-high dilution.

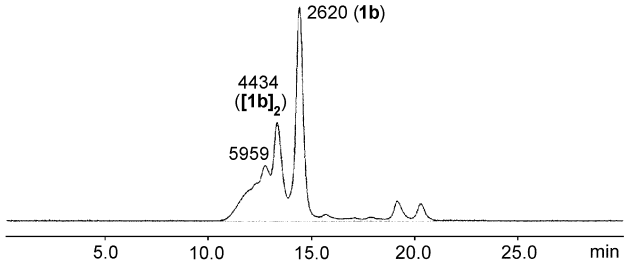

Figure 2. Typical GPC chromatogram of the raw product of a ring closure reaction (of cycle **1b**). The dominant peaks can be assigned to the macrocyle **1b** and cyclic side product [**1b**]$_2$.

Scheme 3. The ring-closure reactions of compounds **20a**−**c** and **21a**,**b** were done under high dilution conditions (ca. 0.0015 M) in sealed vessels as previously described.[15] The product mixture contained the 46-membered macrocycles **1a**−**d**, linear and/or cyclic oligomers (e.g., **[1a]**$_2$−**[1c]**$_2$, the cyclic oligomers with the double molar mass of the corresponding macrocycles **1a**−**c**, see below), and some insoluble material. The raw mixtures were analyzed by GPC, and both the cycle fraction and the next higher molar mass fraction were isolated by preparative GPC (Figure 2). The typical yields for this second fractions were lower than those for the targeted cycles by approximately a factor of 2. The yields of 17−21% of the macrocycles are in the range of what has been described in the literature for similar cycles.[1a,15,16,31] The oligomers may be interesting candidates for studying their potential to form helical secondary structures, a question that is presently of some interest.[32]

Scheme 4. The 58-membered macrocycle **2** with one terpyridine unit was synthesized analogously, i.e., by late assembly of the terpyridine unit. Synthesis and purification of the large terpyridyl percursor **26a** did not cause any problems. The cyclization yield was also in a normal range (18%) despite the considerable increase in cycle size. It is therefore believed that this strategy could be equally well applied to even larger cycles.

Scheme 5 describes a somewhat different strategy for the shape-persistent cycle **3** with two terpyridine units. For one of its two cyclization precursors (**33b**) the terpyridine unit is formed at the latest possible step, similarly to above. The other precursor (**30**) was obtained by coupling **28b** with an excess of the diiodide **29**. The synthesis of the iodo-functionalized half-ring **30** starts from **28a**, which is easily generated by Stille coupling of **10** and **27**. The yield of 70% for the ethynyl-substituted terpyridine **28a** is remarkable. Deprotected terpyridine **28b** is reacted with a large excess of **29** to yield **30**. This suppressed the undesired and difficult to separate off side products. In all cases, no monocoupled side products were detected. Probably, terpyridine compounds that carry free ethynyl units are totally consumed in side reactions (i.e., homocoupling to linear compounds with six pyridine units) during the reaction or workup. Different from **14a** in Scheme 2, the purification of halo-functionalized **30** via column chromatography is not problematic, and most of **29** could be recovered during workup.[31] The same holds true for **35a**,**b** (Scheme 6). Ring closure was carried out under the above conditions and afforded the 46-membered cycle **3** in a yield of 27%.

Scheme 6. From a Sonogashira coupling of terpyridine **33b** with 1,4-diiodobenzene or **34**, the larger iodinated ring precursor **35a** or **35b**, respectively, was synthesized. Ring closure of **33** and **35** under the above conditions led to 58-membered macrocycles **5a**−**c** in yields between 11 and 19%. These somewhat lower yields are probably due to the cycle's lower solubilities leading to a precipitation of product during preparative GPC.

Scheme 7. Finally, the 50-membered macrocycle **4** with two terpyridine units was obtained by Pd^{2+}-catalyzed oxidative ethynyl−ethynyl coupling of **33b**.[23] Also here, the low solubility of the macrocycle in practically all common organic solvents is probably responsible for the low yield. The reaction conditions were therefore not optimized.

Comments Regarding Cycles' Characterization. The characterization of the macrocycles is not complete in all cases because of occasional solubility problems (^{13}C NMR spectra could not be recorded for **3**, **4**, and **5a**,**b**) and sometimes extreme line broadening of the NMR signals. Additionally the chemical shifts in both ^{1}H and ^{13}C NMR spectra sometimes showed a strong concentration and temperature dependence.[1q,6a,13a,14,33]

The MALDI-TOF spectra for **1b**, **1c**, **2**, **3**, **4**, and **5a**−**c** showed the expected signals at m/z = [M + H] or [M + Na/K]. For **1c**, **3**, and **5c** low-intensity peaks, which appeared at higher values, could not be assigned. They do not correlate to open-chain dimers expected from incomplete reaction and may represent either adducts or impurities (not observed by GPC with UV detection). For cycles **1a** and **1d** FAB(+) measurements were done; the structure of these compounds was further proven by X-ray diffraction (see below).

(31) Schmittel, M.; Ammon, H. *Synlett* **1999**, *6*, 750−752.

(32) See, for example: Gong, B. *Chem. Eur. J.* **2001**, *7*, 4336−4342.

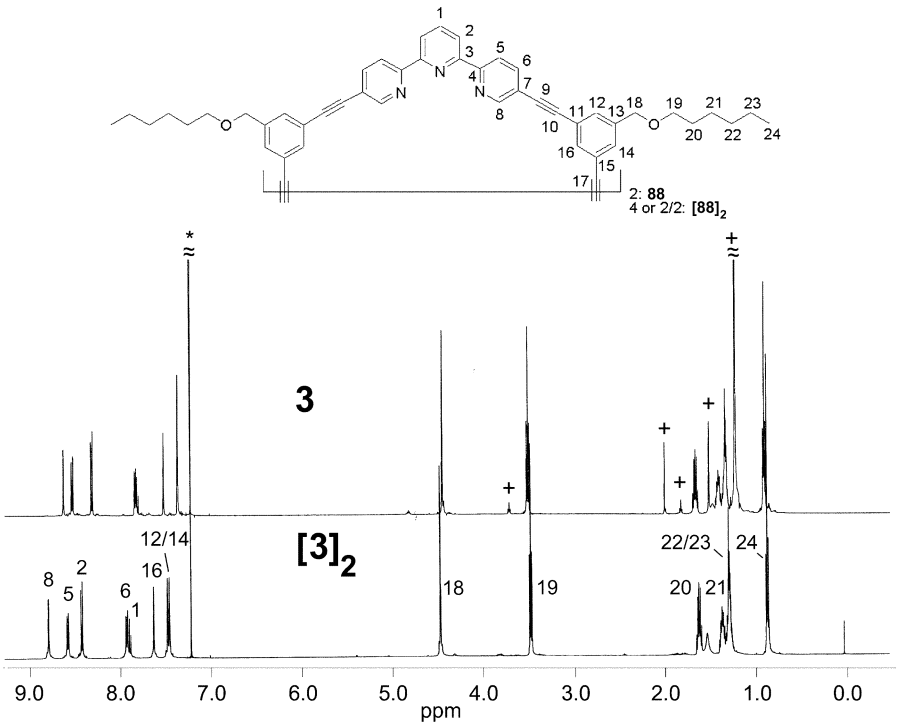

Figure 3. Comparison of the ^{1}H NMR spectra ($CDCl_3$, 500 MHz) of cycle **3** (top) and cyclic side product [**3**]$_2$ (bottom). The numbered peaks were assigned by HETCOR and COSY measurements; + = solvent.

Unfortunately, correct data from elemental analysis could be obtained for neither of the cycles. This was attributed to complexed solvents and/or salts. To produce solvent-free NMR spectra, for example, the samples were treated with deuterated solvents until all protonated solvent was exchanged.

The 58-membered macrocycles with two terpyridine units and only four side chains, **5a** and **5b**, showed extremely broad signals in their ^{1}H NMR spectra. For **5a** when measured in concentrated $CDCl_3$ solutions, signals of the terpyridine unit (8.0−9.0 ppm) broadened so much that they virtually disappeared in the baseline. Upon increasing dilution (not quantified), they could be made visible but were still very broad. The spectrum's resolution could be further enhanced when deuterated trifluoracetic acid was added. The solubility of **5a** improved with decreasing pH. The concentration and pH dependence of the signal broadening are probably due to aggregation; the latter was observed before for similar cycles.[31]

For the remaining 58-membered cycle, **5c**, characterization was much easier, presumably due to its larger number of solubilizing side chains, which not only increased the cycle's solubility but also decreased its tendency to aggregate. If the spectra were recorded directly after sample preparation, well-resolved signals were obtained, and characterization of **5c** by ^{1}H, ^{13}C, and HETCOR NMR spectrometry was allowed.

For all cyclization reactions, defined higher oligomeric fractions could be observed in analytic GPC. For all cycles except **1d**, a second fraction with twice the mass of the dimeric macrocycle was isolated. MALDI or NMR measurements, as far as they could be obtained, prove the cyclic nature of this higher fraction. A definitive decision, whether these cyclic oligomers would be monocycles (from four precursors) or catenanes of two intertwined macrocycles, however, cannot be drawn from these results.[34]

By and large, the characterization of these compounds contained in the second GPC fraction (see Figure 2) was more complicated. They showed a high solubility but unfortunately could not be crystallized into single crystals. From the NMR spectra it was concluded that they do not have end groups and therefore should be cyclic. This was also supported by MALDI-TOF mass spectrometric analyses which showed the expected *m*/*z* values [M + H] and [M + Na/K] for a compound with a double molar mass. Figure 3 shows the ^{1}H NMR spectra of macrocycle **3** and the compound of double molar mass contained in fraction 2. As can be seen, the spectra are very similar in their simplicity and do not show end groups. It is assumed that fraction 2 is the cycle built from four precursors. It cannot, however, be excluded that it has a catenane structure with two intertwined cycles **3**.

Solubility. All ring precursors are well soluble in common solvents such as $CHCl_3$, THF, or toluene. When these compounds are transformed into the more rigid cycles, solubility can be expected to decrease.[35] Quantitative numbers for the solubility of the macrocycles were determined in chloroform, with an additional measurement for **1a** in toluene (Table 1).

For each cycle two measurements were made whose results deviate because of practical problems during measurement. For the poorly soluble cycles, very small amounts had to be weighed. For the well-soluble cycles, the solutions became viscous and extremely difficult to handle, as they tended to dry and precipitate. The average values, therefore, are rough estimates.

(33) See, for example: Lahiri, S.; Thompson, J. L.; Moore, J. S. *J. Am. Chem. Soc.* **2000**, *122*, 11315−11319.
(34) For a work dealing with a similar problem, see: (a) Samorí, P.; Jäckel, F.; Ünsal, Ö.; Godt, A.; Rabe, J. P.*ChemPhysChem* **2001**, *2*, 461−464. (b) Ünsal, Ö.; Godt, A. *Chem. Eur. J.* **1999**, *5*, 1728−1733.
(35) Moore, J. S.; Zhang, J.; Wu, Z.; Venkataraman, D.; Lee, S. *Macromol. Symp.* **1994**, *77* (International Symposium on New Macromolecular Architectures and Supramolecular Polymers **1993**), 295−231.

Table 1. Solubilities of Macrocycles in $CHCl_3$[a]

entry	measured solubility [mg/mL]	average [mg/mL]
1a	4.4, 4.4	~4
1a[a]	7.3, 3.4	~5
1b	388, 247	~300
1d	371, 378	~350
2	>325[b], >225[b]	>300[b]
3	2.5, 2.6	~3
4	7.0, 4.9	~6

[a] Solubility in toluene. [b]Values were measured from an unsaturated solution.

Because of the partially large differences between them, some conclusions can nevertheless be drawn. The most stunning observation is that the cycles are either very poorly (**1a**, **3**, **4**) or extremely well soluble (**1b**, **1d**, **2**). A change in solvent from $CHCl_3$ to toluene has, at least for **1a**, practically no effect.

Three factors were considered to possibly have an impact on the cycles' solubility: number and nature of side chains, number of terpyridine units, and ring size. A cycle carrying a terphenyl unit with one exocyclic hexyloxy side chain (**1a**) has a much lower solubility than the same cycle with a terphenyl unit carrying four hexyl side chains (**1d**). Obviously, the larger the number of flexible chains per cycle, the larger is its solubility. Size, however, does not seem to play an important role. If one compares the 46-membered **1b** and its 58-membered analogue **2**, both of which have the same number of side chains but differ by two phenylacetylene units (ratio ring members/side chains 9.2 for **1b**, 11.6 for **2**), there is practically no difference in solubility.

Terpyridine units generally decrease solubility; cycles with two such units are generally poorly soluble (cf. **1b** with **3**). This is not, as one may think, an incorrect observation due to a smaller number of side chains of **3**. For example, for poorly soluble **3** (with two terpyridine units), the ratio ring members/side chains is 11.5, and the ratio aromatics/side chains is 2.5, while the well-soluble **2** (with one terpyridine unit) has nearly the same values of 11.6 and 2.4, respectively. An influence of the higher symmetry point group of the cycles with two terpyridines (D_{2h}) versus those with one such unit (C_{2v}) cannot be excluded, however.

Perhaps the most interesting observation here results from the comparison of cycles **1a** and **1b**, which differ by a factor of 80 to the advantage of **1b**. The only difference between these cycles is that **1a** carries four hexyloxy side chains in its corners, while **1b** has four hexyloxymethyl side chains. Even if one expects a better solubility in the case of the benzyl ether, where the oxygen is separated from the aromatic and free to rotate, while for the phenol ether, the aromatic−oxygen bond has partially double bond character due to resonance effects, this large effect is astonishing. Other than **3** and **4**, which are nearly insoluble in common solvents even under heating, **1a** dissolves easily in warm THF or benzene but precipitates, however, under cooling.

The ^{1}H NMR spectra of the well-soluble cycles show strong shift dependencies on concentration and temperature. This indicates aggregation, which will be the subject of future investigation.

X-ray Crystallography. Interestingly, there is a striking difference in the tendency of the macrocycles to crystallize. Whereas all attempts to get suitable crystals for an X-ray structure determination of the macrocycles containing two terpyridine units failed, all cycles containing one terpyridine unit (**1a**−**d**, **2**) form nice crystals, and the structure of three of these compounds (**1a**, **1b**, and **1d**) could be determined by X-ray crystallography. This was done at low temperature to prevent disintegration of the crystals by loss of solvate molecules. All three compounds crystallize in the triclinic space group $P\bar{1}$ with one molecule in the asymmetric unit.

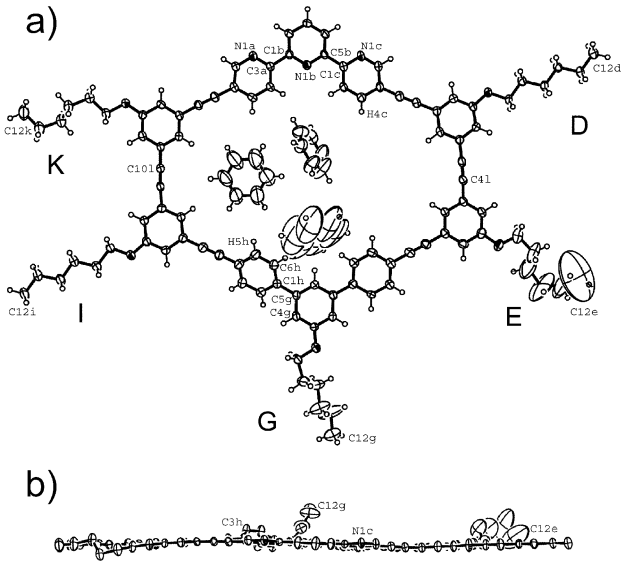

Figure 4. ORTEP[36] diagram of **1a**, 50% probability ellipsoids: (a) view perpendicular to the macrocycle; (b) view parallel to the macrocycle; solvent molecules and hydrogen atoms omitted for clarity.

Although the three systems structurally studied possess the same cyclic backbone, the number and lengths of their side chains and the solvent used for the crystallization have strong effects not only on the crystal packing but also on the distortion of the cycle from planarity. **1a** carries five hexyloxy side chains, and **1b** one hexyloxy and four hexyloxymethyl side chains. This minor difference—together with the fact that **1a** and **1b** were crystallized from different solvents, benzene and toluene, respectively—leads to a significantly different packing, while the backbones of the individual cycles show a similar conformation and form almost planar sheets, as can be seen in a side view of the molecules **1a** and **1b** (Figures 4b and 5b). Cycle **1b**, however, possesses great positional freedom perpendicular to the plane sheet, as expressed by the large thermal ellipsoids. One of the aromatic rings of the terphenyl unit is tilted out of plane (for **1a**, C4g−C5g−C1h−C6h 147.2°, Figure 4a; for **1b**, C6e−C1e−C6d−C5d −149.6°, Figure 5a). As observed in most sterically unrestricted terpyridines, the NCCN torsion angles are close to 180° (for **1a**, N1c−C1c−C5b−N1b 173.7°, N1b−C1b−C3a−N1a −175.6°; for **1b**, N1−C5a−C6a−N2 166.8°, N2−C10a−C11a−N3 178.5°).[20c,37] The data do not allow an unambiguous assignment of the nitrogen atoms, which may even be disordered.

The largest distance across the hole inside the macrocycle is found between the acetylenic carbon atoms (for **1a**, C4l−C10l 1.992 nm; for **1b**, C1c−C7g 1.919 nm). The shortest inner

(36) ORTEP3 for Windows. L. J. Ferrugia, *J. Appl. Crystallogr.* **1997**, *30*, 565.
(37) See, for example: (a) Bessel, C. A.; See, R. F.; Jameson, D. L.; Churchill, M. R.; Takeuchi, K. J. *J. Chem. Soc., Dalton Trans.* **1992**, 3223−3228. (b) Constable, E. C.; Khan, F. K.; Marquez, V. E.; Raithby, P. R. *Acta Crystallogr.* **1992**, *C48*, 932−934.

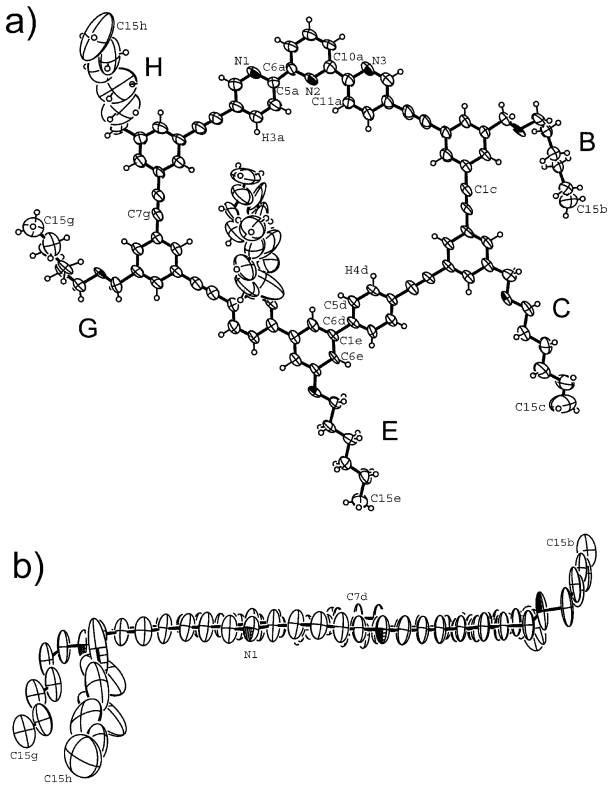

Figure 5. ORTEP[36] diagram of **1b**, 50% probability ellipsoids: (a) view perpendicular to the macrocycle; (b) view parallel to the macrocycle; hydrogen atoms and solvent molecules omitted for clarity.

diameter for **1a** is C4c−C5h 1.248 nm and for **1b** C3a−C4d 1.200 nm. Similar to Moore's all-hydrocarbon phenylacetylenemacrocycles[5b] and our recently published bipyridine-containing macrocycles,[1a,15] both compounds form layered structures.[38]

Compound **1a**·$3C_6H_6$ crystallizes with three molecules of benzene per formula unit. Figure 6a presents a view along 0−1−1 on seven adjacent molecules of **1a** within one layer. Solvate molecules are colored in yellow for clarity. Within the layers the molecules show close contacts at the terpyridine units and four of the five O-hexyl side chains. The almost linear side chain D sticks between the almost linear chain I and chain K of a neighboring macrocycle. Chain K does not show the favorable all-trans conformation of extended alkanes, but is restricted by a neighbored benzene molecule. The chain G leans on one aromatic ring of a terphenyl unit of a neighboring macrocycle. This results in the above-mentioned torsion of the aromatic ring H while all other aromatics are in a plane with the cyclic backbone. The only side chain with no close contact to neighboring molecules within the same layer is chain E, which has interestingly very large thermal parameters and is near the solvate molecules with great positional freedom, as can be seen in Figure 6b. All in all, the packing within one layer reminds one of interacting gear wheels. The remaining free volume is filled with side chains and solvate molecules interlocking adjacent layers. The sides of the cycles overlay in all directions, whereby subsequent layers are shifted against each other (Figure 6b). Removal of the solvent molecules would create channels

(38) For another recent example, see: Höger, S.; Morrison, D. L.; Enkelmann, V. *J. Am. Chem. Soc.* **2002**, *124*, 6734−6736.

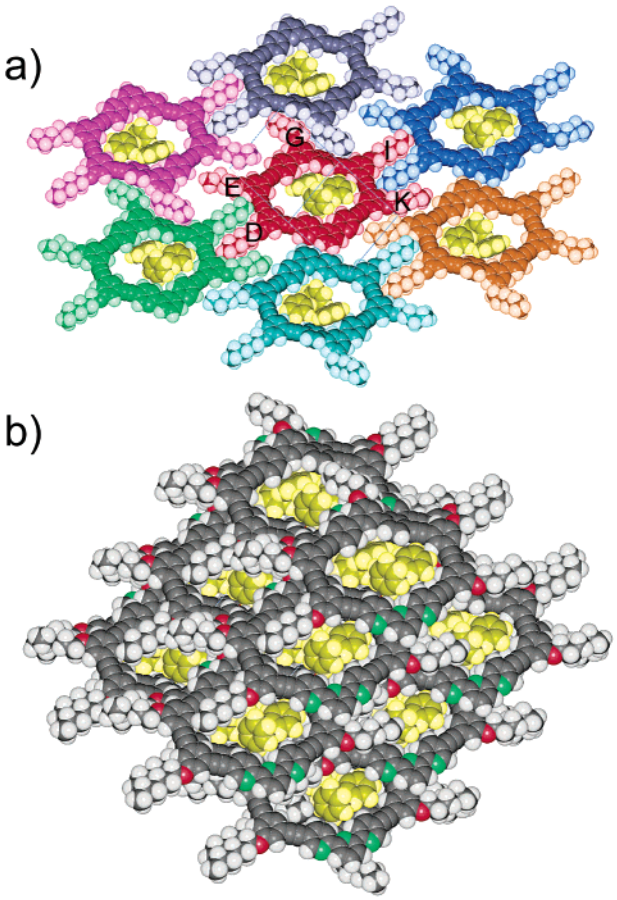

Figure 6. Space-filling model of the packing (SCHAKAL99[39]) of **1a**, view along 0−1−1. Solvent molecules are colored yellow. (a) One layer. Different colors were used to distinguish molecules generated by the following symmetry operations: x, y, z red; $-2+x, 1+y, z$ green; $-x, 2-y, -z$ violet; $2-x, 1-y, -z$ gray; $2+x, -1+y, z$ blue; $2-x, -1-y, 1-z$ orange; $-x, -y, 1-z$ turquoise. (b) Shingle-roof type cut through consecutive layers.

almost along 0−1−1. However, these are not perpendicular to the plane of the molecules.

Compound **1b**·$2C_7H_8$ crystallizes with two molecules of toluene in the asymmetric unit. Figure 7a shows one layer of molecules in a view along the crystallographic *c* axis. Again, the molecules within the layer are in close contact at the terpyridine units, forming parallel "ribbons" of rings at a closest possible distance. These ribbons are held at a distance by interdigitation of the antiparallely oriented two in-plane side chains of each ring (assigned as C and E for one ring). The methyl group of the hexyl chain E turns the benzene ring D out of the macrocycle's plane. Further close contacts are visible at the starting point of chain B. The remaining side chains point above and below the backbone of the macrocycle, linking together adjacent layers, as can be seen in Figure 7b. The side chains H and G are oriented almost perpendicular to the macrocycle's backbone. Chain H, which shows the largest disorder, penetrates the interior of a macrocyclus of the next layer and reaches into the space between the sides of two adjacent macrocycles in the next but one layer; chain G shows opposite behavior.

Compound **1d**·$3C_6H_6$ contains three molecules of benzene per formula unit. The cycle carries eight side chains which do not exclusively point exocyclically. This results in a totally different crystal structure, with the macrocycles, instead of

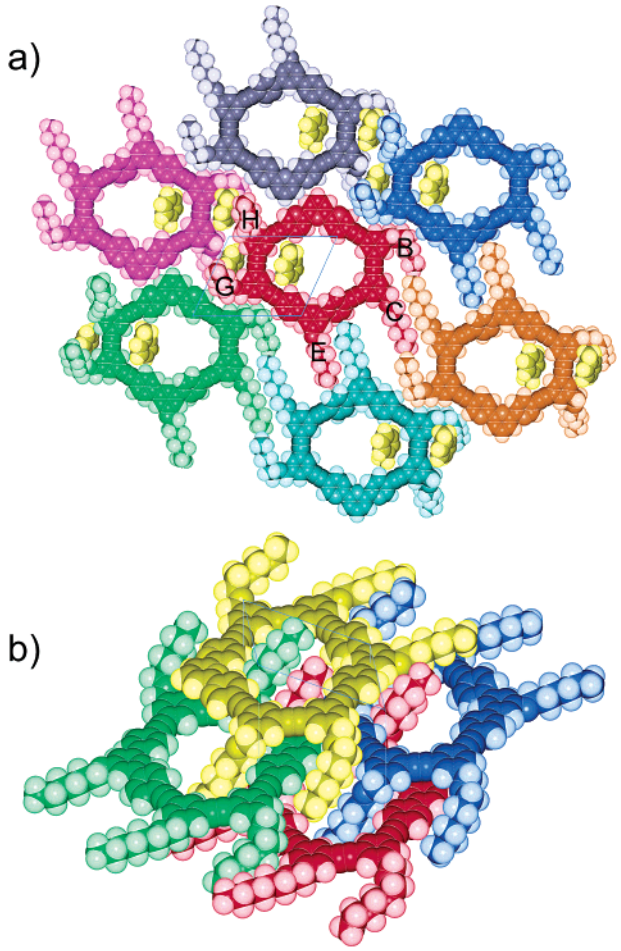

Figure 7. Space-filling model of the packing (SCHAKAL99[39]) of **1b**: (a) view along 0−0−1, solvent molecules colored in yellow for clarity. Different colors were used to distinguish molecules generated by the following symmetry operations: *x*, *y*, z red; −1+*x*, 1+*y*, *z* green; 2−*x*, 2−*y*, 1−*z* violet; 3−*x*, 1−*y*, 1−*z* gray; 1+*x*, −1+*y*, *z* blue; -*x*, −2−*y*, −*z* orange; −1−*x*, −1−*y*, −*z* turquoise; (b) view roughly along 0−1−0, solvent molecules omitted for clarity. Different colors were used to distinguish molecules generated by the following symmetry operations: *x*, *y*, *z* red; 1−*x*, 1−*y*, 1−*z* yellow; −1+*x*, *y*, *z* green; and 2−*x*, 1−*y*, 1−*z* blue.

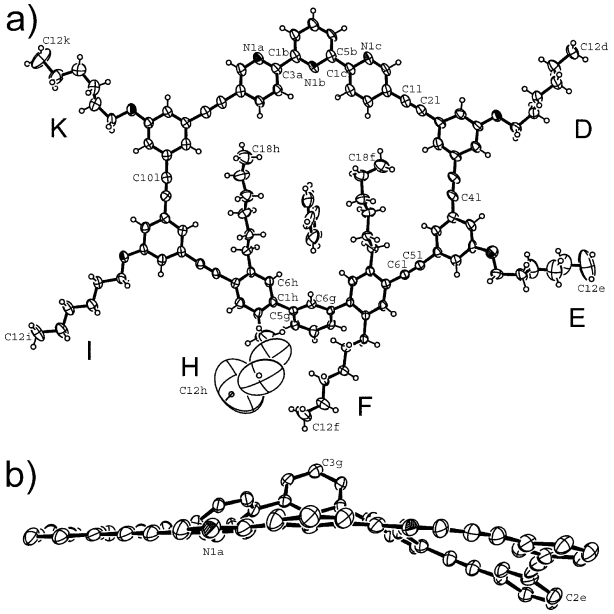

Figure 8. ORTEP[36] diagram of **1d**, 50% probability ellipsoids: (a) view perpendicular to the macrocycle, all but one solvent molecule omitted for clarity; (b) view parallel to the macrocycle; solvent molecules and hydrogen atoms omitted for clarity.

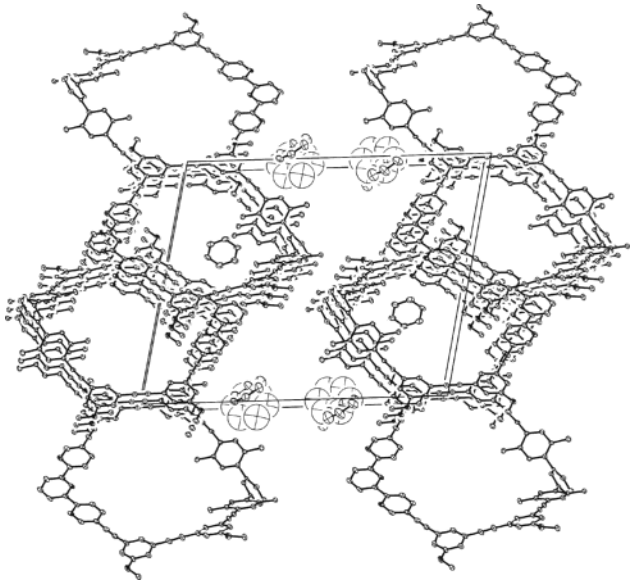

Figure 9. Packing diagram (ORTEP[36]) of **1d**, view along 1−0−0, 20% probability ellipsoids. Side chains and hydrogen atoms were omitted for clarity.

forming planar sheets, being heavily distorted from planarity (C1l−C2l−C5l−C6l 25°, C6h−C1h−C5g−C6g 70°, Figure 8). The inner diameters, however, are quite well in accordance with those of **1a**,**b** (C4l−C10l 1.840 nm, C4c−C5h 1.343 nm), and this holds true also for the terpyridine conformation (N1a−C3a−C1b−N1b 176.2°, N1b−C5b−C1c−N1c −171.1°).

The packing follows a more simple AB layer pattern along the *a* axis and differs from the other cycles because there is overlap between the cycles only in the direction of the *b* axis (Figure 9). Thus macrocyclic backbone and side-chain areas alternate along the *c* axis. Within the side-chain area remain two neighboring channels which are shared by the most highly disordered components of the structure. They are filled with the two benzene solvate molecules per formular unit, which lie roughly perpendicular to each other and are separated by the outer side chain F. One solvate molecule has extremely large thermal parameters and thus great positional freedom. The inner F and H side chains stretch through the interior space of the cycle with one benzene molecule sandwiched between them. One K chain from a cycle of the next layer also reaches into the cycle. The remaining side chains pack into the space between the cycles.

Scanning Tunneling Microscopy. While much endeavor has been addressed recently to understanding and controlling the physisorption of phenylene-based rodlike and disklike molecules into ordered nanostructures at the solution−HOPG (highly oriented pyrolitic graphite) interface,[40] only few studies have been reported on the formation of ordered architectures of

(39) SCHAKAL: E. Keller, *J. Appl. Crystallogr.* **1989**, *22*, 12−22.
(40) (a) Samorí, P.; Fechtenkötter, A.; Böhme, T.; Jäckel, F.; Müllen, K.; Rabe, J. P. *J. Am. Chem. Soc.* **2001**, *123*, 11462−11467. (b) Samorí, P.; Severin, N.; Müllen, K.; Rabe, J. P. *Adv. Mater.* **2000**, *12*, 579−582. (c) Stabel, A.; Herwig, P.; Müllen, K.; Rabe, J. P. *Angew. Chem., Int. Ed. Engl.* **1995**, *34*, 303−307. (d) Askadskaya, L.; Boeffel, C.; Rabe, J. P. *Ber. Bunsen-Ges. Phys. Chem.* **1993**, *97*, 517−521. (e) Rabe, J. P.; Buchholz, S. *Phys. Rev. Lett.* **1991**, *66*, 2096−2099.

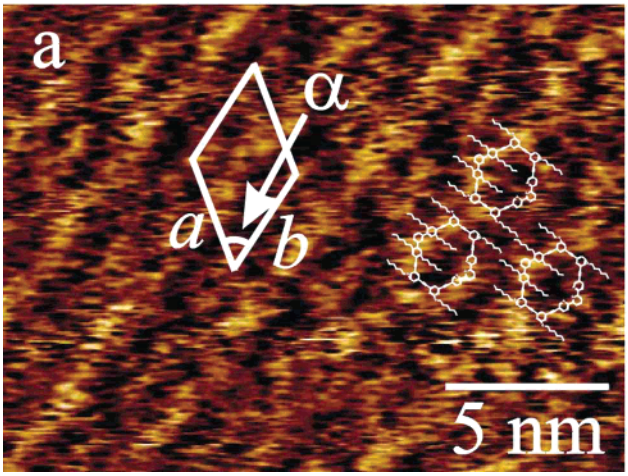

Figure 10. STM image of compound **1d** recorded in current mode at the solution−HOPG interface. Tunneling parameters $U_t = 640$ mV, $I_t = 36$ pA.

conjugated macrocycles that were based on phenylene−ethynylene[6a] or thiophene units.[1d,6b,41] Also taking into account that little is known regarding the self-assembly at surfaces of pyridine-based conjugated systems,[42] we have considered it most important to extend our exploration on the aforementioned pyridine-based macrocycles to their behavior in ultrathin films. The STM investigations have been executed at the solution−HOPG interface on macrocycles **1d**, **5a**, and **5c**. Among these three different macrocycles investigated, only compound **1d** could physisorb into highly ordered nanostructures at the solution−HOPG interface. The STM current image is shown in Figure 10. In the same figure the unit cell of the molecular arrangement and the model of the packing are superimposed. The adsorbate unit cell possesses an oblique geometry: it amounts to $a = 3.7 \pm 0.2$ nm, $b = 3.5 \pm 0.2$ nm, $\alpha = 54 \pm 3°$.

The contrast in the STM current images is mainly ruled by the difference between the energies of the molecular states of the adsorbate and the Fermi level of the substrate. Thus, due to a larger energy difference, aliphatic chains on HOPG generally appear darker than moieties with π-electrons, provided that the moieties are lying equally flat on the substrate.[34a] In our example of a three-dimensional (non perfectly flat) object, the contrast depends additionally on the degree of spatial overlap of the electronic states of the adsorbate with those of the substrate.[40a,43]

In view of these facts, one can try to interpret the observed contrast in the current STM images displayed in Figure 10. An angular bright segment is visible and can be ascribed to the terphenylene unit. With a slightly lighter contrast, in the positions that are placed at the edges of the drawn unit cells, the unsubstituted terpyridine segments are located. Their lower contrast, if compared to the terphenylene units, can be explained with both the different electronic structure of the moiety and a different coupling with the substrate's electronic states. This latter effect would be due to a diverse location along the *z* axis of the conjugated orbitals with respect to the HOPG states. In particular, the fact that the contrast of the terpyridine segments is not elongated but rather appears as a spherical spot suggests that the two external pyridine rings are nonplanar with respect to both the central one and to the basal plane of the HOPG surface. The alkoxy and alkyl side chains are likely to be arranged according to a 2-fold symmetry, as observed for other "hairy disks".[40c,d] In the present case, the high conformational mobility at the surface, which occurs on a time scale faster than the scanning frequency, and/or their electronic states, which are far away from the Fermi level of the HOPG, did not allow us to resolve their structures. The overall molecular arrangement on the surface of graphite is loosely packed. This means that the gain in enthalpy upon adsorption on HOPG is not very high.[40a] This is most likely the reason for the low stability in time of the visualized 2D crystals which indeed revealed a high dynamics in the seconds time scale. Moreover, the nonplanar conformation, which has been observed by X-ray diffraction in the crystal of **1d**, makes its adsorption at surfaces expensive from an entropy viewpoint, since a planarization needs to occur.

Ordered nanostructures of **5a** and **5c** could not be observed on HOPG. The reason for this might be found in the thermodynamics of the physisorption at the solid−liquid interface. These two macrocycles are bigger than **1d** and consequently have a larger cavity in the middle. This larger hole represents a lack in enthalpy gain, which is one basis for the physisorption at surfaces. As already noticed for **1d** the low stability could be ascribed to a low gain in enthalpy. Upon increasing the size of the macrocycles, this enthalpic gain becomes too small to overcome the loss in entropy associated with transition from the 3D of a solution to the 2D of the surface and to the translational entropy needed to create a tightly packed supramolecular architecture at surfaces.

Conclusions

A set of large terpyridine-containing macrocycles with 46 (**1a**−**d**, **3**), 50 (**4**), and 58 atoms (**2**, **5a**−**c**) in the cyclic core was synthesized using a flexible building block approach. This approach allowed one to systematically vary the cycles' sizes and side-chain patterns and has the potential to be applied to even larger cycles. In most cases it proved best to generate the terpyridine units at a late stage of the synthetic sequence. The macrocycles' solubility, a significant factor for both their handling and characterization, is strongly influenced by even minor variations in the cycles' side-chain pattern. The three cycles **1a**, **1b**, and **1d** could be grown into single crystals and their structures solved by low-temperature X-ray diffraction. They form layered structures, and the cycles of consecutive layers form columnar stacks that are filled with solvent molecules and flexible side chains. The respective detailed packing strongly depends on the side-chain pattern. Apart from cycles **1a** and **1b**, whose cores are planar, cycle **1d** in the crystal significantly deviates from the planar geometry. Monolayers of this cycle on HOPG were investigated by STM. Though the resolution of the images obtained is not very high, a packing model for this "2D crystal" could nevertheless be derived. Both the image's nonoptimal resolution and the monolayer's low stability in time were attributed to **1d**'s presumed relatively low adsorptive attraction on HOPG, which may be caused by preferred nonplanar conformations as they were observed in the single crystal.

(41) Mena-Osteritz, E.; Bäuerle, P. *Adv. Mater.* **2001**, *13*, 243−246.
(42) (a) Ziener, U.; Lehn, J.-M.; Mourran, A.; Möller, M. *Chem. Eur. J.* **2002**, *8*, 951−957. (b) Semenov, A.; Spatz, J. P.; Möller, M.; Lehn, J.-M.; Sell, B.; Schubert, D.; Weidl, C. H.; Schubert, U. S. *Angew. Chem., Int. Ed.* **1999**, *28*, 2547−2550.
(43) Lazzaroni, R.; Calderone, A.; Brédas, J. L.; Rabe, J. P. *J. Chem. Phys.* **1997**, *107*, 99.

Experimental Section

Synthesis. Compounds **6**,[29a] **10**,[27] **12b**,[15] **16b**,[15] **22**,[29a] **29**,[29b] and **34**[44] were prepared according to literature procedures. For the synthetic procedures and analytical data for all other compounds, please see the Supporting Information.

Solubility Measurements. Concentrated solutions of the compounds were gained by shaking an excess of material in $CHCl_3$ or toluene overnight. After filtration, defined volumes (ca. 0.5−1 mL for the less soluble, ca. 0.01 mL for the better soluble substances) were transferred with an Eppendorf pipet to a probe glass, the solvent was evaporated, and the residue was dried in high vacuum and weighed.

X-ray Analysis. Crystals of **1a** suitable for X-ray crystallography were obtained by crystallization from hot benzene. Attempts to get suitable crystals from THF or toluene failed. Compounds **1b** and **1d** are considerably more soluble than **1a** in common solvents and crystallize less readily. Crystals were obtained by slow diffusion of methanol into a solution in toluene (for **1b**) or benzene (for **1d**) at ambient temperature.

As all three compounds crystallize with solvent molecules and therefore tend to disintegrate with loss of the included solvate, the crystals were mounted out of saturated solutions at low temperature on the top of a glass fiber and the data collection was performed at low temperature using a Bruker-AXS SMART CDD diffractometer. A total of 600 frames ($\Delta\omega = 0.3°$) for each run were collected for three ϕ positions (0°, 90°, and 240°), resulting in 1800 frames for each data set. The data were reduced to F_o^2 and corrected for the absorption effects using SAINT[45] and SADABS,[46] respectively. The structures were solved using direct methods (SIR92[47] **1a** and **1b**, and SHELXS[48] **1d**) and refined using full matrix least squares (SHELXL 97[48]).

All non-H atoms were refined anisotropically. The hexyl side chains were refined with the help of similar distance restraints for the 1,2 and 1,3 bond distances as well as rigid bond restraints for the anisotropic replacement parameters. The aromatic rings of **1b** and the solvent molecules of all compounds were refined as rigid bodies. The hydrogen atoms were included at geometrically calculated positions and refined using a "riding model" with isotropic thermal parameters (U(H) = 1.5U_{eq}(C) for methyl groups and U(H) = 1.2U_{eq}(C) for all other H atoms). Crystal data, experimental conditions, and refinement values are listed in the Supporting Information. ORTEP[36] for Windows and SCHAKAL99[39] were used for preparing the graphical representations. The molecular structures of **1a**, **1b**, and **1d** are depicted in Figures 4, 5, and 8. Packing diagrams are presented in Figures 6, 7, and 9.

STM Investigation. Almost saturated solutions of the macrocycles **1d**, **5a**, and **5c** in 1,2,4-trichlorobenzene were applied to the basal plane of a freshly cleaved HOPG surface. By changing the tunneling parameters during the STM imaging, namely, the voltage applied to the tip (U_t) and the average tunneling current (I_t), it was possible to switch between the visualization of the adsorbate layer to that of the underlying HOPG substrate with a lattice resolution. This enabled us to calibrate the images of the molecular adsorbate with respect to the underlying HOPG.

Scanning tunneling microscopy investigations were carried out using a picoAmp-Nanoscope IIIa (Digital Instruments), which allows the detection of a tunneling current of 1 pA. This latter characteristic is an essential prerequisite for studying in a noninvasive way organic layers that are known to be poorly conductive. Images were recorded with a scan rate of ca. 13−18 line/s with a resolution of 512 × 512 pixels. The Pt/Ir (85%, 15%) STM tips were prepared by electrochemical etching.

Acknowledgment. This work was supported by the Deutsche Forschungsgemeinschaft (Sfb 448, TPs A1 and B5) and the Fonds der Chemischen Industrie. We thank Ms. E. Franzus and Dr. G. Holzmann for their competent help with EI and FAB mass spectrometric analyses and Ms. C. Zimmermann for her help with GPC analyses.

Supporting Information Available: Synthetic procedures and analytical data for the compounds prepared; X-ray crystallographic files in CIF format for compounds **1a**, **1b**, and **1d**. This material is available free of charge via the Internet at http://pubs.acs.org.

JA034029P

(44) Hensel, V. Ph.D. Thesis, FU Berlin, Germany, 1998.
(45) *SAINTPLUS* Software Reference Manual, Version 5.054; Bruker-AXS: Madison, WI, 1997−1998.
(46) Blessing, R. H. *Acta Crystallogr., Sect. A* **1995**, *51*, 33−38. *SADABS*; Bruker AXS, 1998.
(47) *SIR92*, A program for crystal structure solution: Altomare, A.; Cascarano, G.; Giacovazzo, C.; Guagliardi, A. *J. Appl. Crystallogr.* **1993**, *26*, 343−350.
(48) Sheldrick, G. M. *SHELX97* [includes *SHELXS97*, *SHELXL97*, *CIFTAB*], Programs for Crystal Structure Analysis (Release 97-2); Institut für Anorganische Chemie der Universität: Tammanstr. 4, D-3400 Göttingen, Germany, 1998.